



Impacts of the 1.5 °C global warming target on future burned area in the Brazilian *Cerrado*



Patrícia S. Silva^a, Ana Bastos^b, Renata Libonati^{c,a,*}, Julia A. Rodrigues^c, Carlos C. DaCamara^a

^a Instituto Dom Luiz, Faculdade de Ciências, Universidade de Lisboa, Lisboa, Portugal

^b Ludwig-Maximilians-Universität München, Germany

^c Departamento de Meteorologia, Instituto de Geociências, Universidade Federal do Rio de Janeiro, Rio de Janeiro, Brazil

ARTICLE INFO

Keywords:

Climate change
Brazil
Regional climate model
Reanalysis
Fire danger
Future burned area

ABSTRACT

Worldwide, fires have substantial economic, social and health-related impacts. Brazil is one of the most affected areas in the globe, particularly the *Cerrado*, a savanna-like biome, whose composition, structure, species abundance and diversity are shaped by recurring fires. The aim is to assess present and future trends of fire danger and burned area (BA), using the Daily Severity Rating (DSR), an extension of the Canadian Forest Fire Weather Index System, and climate outputs from a regional climate model, the RCA4 from the Rossby Centre. To that end, we validated the climate variables simulated by RCA4 and the resulting DSR, both showing consistency with observation-based datasets. We then developed a statistical model of BA using fire season averaged DSR as a predictor, found to explain 71% of the interannual variability of BA from 2003 to 2017. Using the statistical model, we projected future fire danger and BA over *Cerrado* for IPCC Representative Concentration Pathways 2.6, 4.5 and 8.5. Results show an increase in future BA for all scenarios, with pronounced changes for RCPs 4.5 and 8.5, where BA is expected to increase by 39% and 95% for 2100. In the case of RCP 2.6, the closest scenario to the 1.5 °C target established by the United Nations, results indicate an increase in mean BA up to 22% by 2050, compared to the historical period, followed by a decrease to 11% by 2100. This is especially relevant since RCP 2.6 is the only scenario where such a decrease is projected, highlighting the importance of keeping global mean surface temperature below the 1.5 °C warming target.

1. Introduction

Several studies have underlined the link between fire activity and climate change (Flannigan et al., 2013; Gillett et al., 2004; Westerling et al., 2006) and fire is arguably the most important disturbance agent in terrestrial ecosystems at a global scale, releasing every year significant amounts of carbon to the atmosphere (2.2 PgC/yr; van der Werf et al., 2017). Estimates of global annual burned area (BA) range from 300 to 450 Mha (Chuvieco et al., 2016; Flannigan et al., 2013; van der Werf et al., 2017). Fires have substantial impacts on ecosystem structure and distribution, energy budget, biogeochemical cycles, atmospheric chemistry and composition, as well as on human health and the economy (DeBano et al., 1998; Kozłowski et al., 1974).

Although often perceived as a natural hazard whose consequences are mainly negative, e.g., by destroying ecosystems and endangering populations, fire is a natural part and plays a key regulating role in many environments (Bond and Keeley, 2005; Bowman et al., 2009; Pivello, 2011). For instance, fire clears the dead litter on forest floors which allows important nutrients to return to the soil, creating

favourable conditions for animals and plants to develop. Fire-dependent biomes, such as the Brazilian savanna (*Cerrado*), are those that regularly burn constrained to the annual and seasonal climatological conditions, fuel accumulation, among other influencing factors (Hardesty et al., 2005). Growing under hot and seasonally dry climatic conditions, *Cerrado* is characterized by high fire weather susceptibility, where pre-fire vegetation conditions are strongly influenced by climate and determine the intensity and severity of the burning (Dantas et al., 2013a; Hoffmann et al., 2012b). The persistence and seasonality of fire weather danger in the *Cerrado* are therefore related to the marked contrast between wet/humid seasons (Nogueira et al., 2017) and led to several species developing adaptations to fire for seed germination and colonization (Miranda et al., 2009).

Although fire is a natural disturbance in *Cerrado*, its behaviour is strongly influenced by human activity (Hantson et al., 2015). Land cover and land use changes have disrupted natural fire patterns and the resulting feedbacks with climate and vegetation (Wu et al., 2017). Changes in fire regimes by human activity (either directly, through land use practices, or indirectly, through changes in climate) can also have

* Corresponding author.

<https://doi.org/10.1016/j.foreco.2019.05.047>

Received 28 January 2019; Received in revised form 15 May 2019; Accepted 16 May 2019

Available online 21 May 2019

0378-1127/ © 2019 Elsevier B.V. All rights reserved.

substantial impacts affecting community distribution (Kozłowski et al., 1974; Schmidt et al., 2018) and trait variability (Dantas et al. 2013b; Hoffmann et al., 2012a). They can further lead to increased woody encroachment (Hoffmann, 1999) and establishment of invasive grasses (Durigan et al., 2007; Gorgone-Barbosa, 2016). Therefore, altered fire regimes in *Cerrado* can profoundly change this biome, as its species are not merely adapted to fire but rather to a set of environmental conditions that encompass the fire regime. Conversely, fire's beneficial effects in fire-prone regions can only occur if the fire does not burn for too long or with too high intensity. Quantifying long-term changes in the temporal and spatial patterns of fire occurrence in *Cerrado* is therefore crucial for understanding the driving forces of changes in fire patterns (Gomes et al., 2018).

Substantial efforts have been made to model present and future fire distribution in several regions of the globe, towards an increased understanding of their impacts on ecosystems (Bradstock, 2010; Carvalho et al., 2011; Chen et al., 2011; Hantson et al., 2016; Pausas and Ribeiro, 2013; Silva et al., 2016). In this context, Global Climate Models (GCMs) play a crucial role because they can provide estimates of the evolution of the climate variables that influence fire activity in the coming decades. Earth System Models (ESMs) further include biogeochemical processes and some explicitly simulate fire. However, it has been shown that there is little agreement between models on how fire evolved in the past or will change in the future (Kloster and Lasslop, 2017). Although GCMs and ESMs have been increasing in complexity, their low spatial resolution may hamper an accurate representation of regional processes and forcings relevant for fire, including topography and other land-surface characteristics (Rummukainen, 2010). Consequently, they may lack the detail required to study and evaluate the effects of climate change at regional scales that are particularly important when analysing extreme events. To tackle this limitation, regional climate models (RCMs) have been developed. RCMs operate at much finer scales and use GCM fields, such as greenhouse gases (GHG) concentrations or the radiative forcing, as boundary conditions; they provide a wide range of meteorological variables which can be used to estimate fire danger with finer detail.

Here we perform a systematic analysis of the outputs of one RCM from the CORDEX project (Giorgi et al., 2009) to assess present and future patterns of fire danger and BA over the Brazilian *Cerrado*. Fire danger is here interpreted as the likelihood that climate conditions prone for fire ignition and spread are observed and may be used as a guide to predict future fire behaviour in the absence of fire management and help stakeholders make informed decisions on fire mitigation strategies. The analysis is made using the Daily Severity Rating (DSR), an extension of the Canadian Forest Fire Weather Index (FWI) System that is a highly adaptable fire danger index system, proven to work in distinct ecosystems worldwide (Nogueira et al., 2017; Pinto et al., 2018; Taylor and Alexander, 2006). We first evaluate the capability of the DSR, calculated using observation-based climate, to accurately track the patterns and trends of satellite-derived BA over Brazilian *Cerrado* in recent decades. A linear regression model linking DSR and BA is then developed using observation-based data and recorded burned areas covering the period 2003–2017. We then test the applicability of DSR as estimated from RCM outputs. The linear burned area statistical model (BAM) is applied to the RCM outputs for recent past climate conditions (1981–2005), and a calibration is performed so that the statistical distributions of obtained BA estimates are the same as the observed BA. Finally, future fire danger and the expected impacts on the burned area are estimated by applying the calibrated statistical model to RCM outputs respecting to a wide range of possible changes in future anthropogenic GHG concentration using IPCC's Representative Concentration Pathways (RCP) (IPCC, 2013).

2. Data and methods

2.1. Meteorological parameters

Values of daily surface temperature (T), relative humidity (RH),

precipitation (P) and wind (W) were retrieved for South America for both observation-based and simulated data, over different periods as described below.

2.1.1. Climate reanalyses

Daily observation-based data for the period 1980–2017 comprehend three third-generation reanalyses products: (i) the European Centre for Medium-Range Weather Forecasts' (ECMWF) ERA-Interim reanalysis (Dee et al., 2011); (ii) the Japanese 55-year Reanalysis (JRA-55) from the Japan Meteorological Agency (JMA) (Kobayashi et al., 2015); and (iii) the National Aeronautics and Space Administration's Global Modelling and Assimilation Office (NASA/GMAO) MERRA-2 reanalysis (Gelaro et al., 2017). ERA-Interim uses the ECMWF Integrated Forecast Model (IFS Cy31r2), and the data assimilation scheme is based on a 12-hourly four-dimensional variational analysis (4D-Var). The model uses 60 vertical levels with the top of the atmosphere at 0.1 hPa, and its spectral resolution is T255 (≈ 80 km). JRA-55 is produced with the TL319 version of JMA's operational data assimilation system based on a 6-hourly 4D-Var analysis, performed with a T106 inner model (≈ 55 km) that uses 60 levels up to 0.1 hPa. Lastly, MERRA-2 uses the new and improved version of the Goddard Earth Observing System data assimilation system version 5 (GEOS-5), on a cubed sphere grid, with $\frac{1}{2}^\circ$ latitude by $\frac{5}{8}^\circ$ longitude ($\approx 55 \times 70$ km) resolution and 72 vertical levels from the surface to 0.01 hPa, based on a 6-hourly three-dimensional variational (3D-Var) scheme.

Several studies have explored the differences between these reanalyses and how their respective physical processes are described (Auger et al., 2018; Bosilovich et al., 2008; Brunke et al., 2011; Kim et al., 2018; Trenberth et al., 2011). Overall, the three observation-based datasets produce varying results according to their different data assimilation schemes, providing a range of admissible results that allow better assessing the consistence of the outputs of the RCM with reanalyses.

2.1.2. RCM outputs

Simulation outputs of present and future climate are obtained from the regional downscaling of EC-Earth for the South American domain of the CORDEX experiment, performed by the Rossby Centre using RCA4 as the atmospheric model (Strandberg et al., 2014). The EC-Earth is a coupled global climate model based on the operational seasonal forecast system of the ECMWF (Hazeleger et al., 2012), used in the Coupled Model Intercomparison Project Phase 5 (CMIP5). EC-Earth outputs were used as boundary conditions for the RCA4 regional climate model. RCA4 is based on the numerical weather prediction model HIRLAM and is thoroughly described in Samuelsson et al. (2011). The model includes improved land surface processes compared to its previous version, such as the lake model and physiography (Samuelsson et al., 2015); however, it is worth noting that the mask for the land-sea and the fractions of lakes/forests remain static throughout the calculations and that the regional model does not simulate fire nor changing vegetation. Both regional and global climate models have shown satisfactory results in representing several components of the climate system, in particular, temperature and precipitation (Dieterich et al., 2013; Falco et al., 2018; Iqbal et al., 2017; Menéndez et al., 2019; Solman and Blázquez, 2019; Sterl et al., 2012).

Daily values of near-surface air temperature, near-surface relative humidity, near-surface wind speed, and precipitation were obtained at a spatial resolution of $0.44^\circ \times 0.44^\circ$ (approximately 50 km). Four distinct experiments were used, one corresponding to the historical period for the model and index validation (1976–2005), and the remaining three corresponding to the IPCC's RCP 2.6, 4.5 and 8.5 for the 21st century (IPCC, 2013). RCP 2.6, 4.5 and 8.5, correspond, respectively, to stringent mitigation and mild and severe climate change scenarios. RCP 2.6 is the closest to the goal of 1.5 °C global mean surface temperature warming compared to pre-industrial levels set in the 21st session of the Conference of the Parties (COP21) in Paris, December 2015 (Masson-Delmotte et al., 2018; UNFCCC, 2015).

2.2. Burned area

Burned area is estimated based on the *Área Queimada* MODIS Collection 6 1 km (AQM) product, specifically developed for Brazil by Libonati et al. (2015) and disseminated by the INPE's Fire Monitoring Team website. Data are provided in grid cells of 1 km by 1 km and cover a 15-year period (2003–2017). AQM estimates of BA are obtained using a burn-sensitive vegetation index based on top-of-the-atmosphere values of middle infrared radiance and near-infrared reflectance, acquired by the MODIS instrument on board NASA's Terra and Aqua satellites (DaCamara et al., 2016; Libonati et al., 2011). Available by the end of 2018, AQM Collection 6 includes updated calibration and geolocation information from MODIS Collection 6 in addition to algorithm updates. According to INPE's Fire Monitoring Team, AQM Collection 6 also incorporates corrections of non-homogeneities related to post-processing quality flags. This improved procedure reflects on the inter and intra-annual patterns of variability of BA in *Cerrado* that are different from the ones in previous studies (Fidelis et al., 2018).

When compared with MODIS burnt area products (MCD45A1 and MCD64A1) for Brazil, AQM shows increased performance and better agreement with high-resolution LANDSAT data, with noticeable results for the *Cerrado* region where burned pixels were identified with a lower number of omission errors (Libonati et al., 2015). The AQM dataset has also been successfully used to study the Amazonian forest-savanna (Wuyts et al., 2017).

The MODIS Burned Area Product MCD64 Collection 6 (Giglio et al., 2018) was also employed for validation purposes. The product relies on daily surface reflectance dynamics to detect the approximate date of burning and map the spatial extent of fires from 2001 to 2017 (Giglio et al., 2016).

2.3. Fire danger index

In this study, meteorological fire danger is assessed using the FWI system, that consists in six components accounting for the effects of fuel moisture and wind on fire behaviour (Van Wagner, 1987). All components of the FWI system are computed using daily values at 18:00 UTC (about 15:00 local time) of T, RH and W, and 24-hour P. Directly derived from the FWI system, the Daily Severity Rating (DSR) provides a numeric rating of the difficulty of controlling fires, reflecting the expected efforts required for fire suppression.

2.4. Region of interest

This analysis will focus on *Cerrado* (Fig. 1), the dominant vegetation of central Brazil covering about 25% of the country, with an estimated area of approximately 2 million km² (Durigan and Ratter, 2016). *Cerrado* is one of the most important global biodiversity hotspots (Myers et al., 2000), with over 13 thousand species recorded, a similar number to that registered for the Amazon rainforest (Overbeck et al., 2015). As the primary agricultural frontier of Brazil, *Cerrado* is the main contributor to Brazil's annual BA (Programa Queimadas INPE, 2018) and, although fire occurs naturally in this biome, the fire regime has been changing in frequency, severity, extent, and seasonality (Shlisky et al., 2008). The AQM product estimates that, over a 15-year period from 2003 to 2017, *Cerrado* represented 51% of Brazil's total burned area.

2.5. Data pre-processing

Daily values of observation-based DSR are computed for 1981–2017 at each grid point using T, RH, W and P data from the three reanalyses (ERA-I, MERRA-2, and JRA-55). For each reanalysis dataset, monthly means of DSR were obtained by averaging the corresponding daily values, and then spatially averaging over grid points belonging to *Cerrado*. The same procedure was applied to simulation-based DSR from the RCA4 model in order to obtain the respective values for the

historical period (1976–2005) and for RCPs 2.6, 4.5 and 8.5, in two 30-year periods, ending in the first half (2021–2050) and in the second half (2071–2100) of the 21st century. According to the IPCC, relative to 1850–1900, global surface temperature change for the end of the 21st century (2081–2100) is unlikely to exceed 2 °C for RCP2.6, more likely than not to exceed 2 °C for RCP4.5 and likely to exceed 2 °C for RCP8.5 (IPCC, 2013).

Finally, for both AQM and the MCD64 products, monthly cumulated values of BA over *Cerrado* were obtained by spatially aggregating monthly BA values over 2003–2017.

2.6. Statistical analysis

Following Pereira et al. (2013), the burned area model is built by performing a linear regression on time series of DSR (predictor) and the decimal logarithm of BA (predictand):

$$\log_{10}(BA) = mDSR + b \quad (1)$$

where m and b are the slope and intercept of the model.

Goodness of fit of the linear model is evaluated using the coefficient of determination and, given the short length of the time series, effects of overfitting are assessed by the decrease in the coefficient of determination after applying a leave-one-out cross-validation scheme (Wilks, 2011) for the 15 years of data. Moreover, to evaluate the statistical significance of the DSR-BA correlation, 10,000 random ranks of DSR and BA are simulated from 2003 to 2017 using a Monte Carlo approach and their corresponding coefficients of determination estimated.

Using the maximum likelihood method, normal distributions are fitted to the time series of observed and simulated DSR, and Lilliefors tests (Lilliefors, 1967) are used to test the null hypothesis that data come from a normally distributed population with unknown mean and standard deviation.

Let DSR_{ERA-I} (DSR_{hist}) denote the values of DSR as derived from observation-based ERA-I data (from RCA4 data for the historical period). DSR_{hist} is then calibrated so that the fitted normal distribution has the same mean and standard deviation than DSR_{ERA-I} . The calibration process is based on the fact that a variable X_1 with a normal distribution with mean μ_1 and standard deviation σ_1 is converted into a variable X_2 with a normal distribution with mean μ_2 and standard deviation σ_2 using the following transformation:

$$X_2 = \frac{X_1 - \left(\mu_1 - \frac{\sigma_1}{\sigma_2}\mu_2\right)}{\frac{\sigma_1}{\sigma_2}}, \quad \text{where } X_1 \sim N(\mu_1, \sigma_1) \text{ and } X_2 \sim N(\mu_2, \sigma_2) \quad (2)$$

Calibrated values of DSR_{hist} are accordingly obtained by applying (2) to DSR_{ERA-I} , with μ_1 and σ_1 (μ_2 and σ_2) being the mean and standard deviation obtained when fitting normal models to DSR_{ERA-I} (DSR_{hist}). Projected values of DSR for the two periods of the 21st century (2021–2050 and 2071–2100) are then corrected by applying to the respective time series the transformation that was used to calibrate DSR_{hist} . This procedure is only applied in Section 3.4, after showing the need for calibrating DSR (Section 3.3).

The following transformation is applied to estimate the mean and standard deviation of the distributions of BA for the historical period and future climate scenarios. Assuming that $DSR \sim N(\mu_{DSR}, \sigma_{DSR})$, then taking into account (1):

$$\log_{10}(BA) \sim N(\mu', \sigma') \text{ with } \mu' = m\mu_{DSR} + b \text{ and } \sigma' = m\sigma_{DSR} \quad (3)$$

Moreover, given that $\ln BA = \log_{10}(BA)/\log_{10}(e)$, we obtain:

$$\ln(BA) \sim N(\mu, \sigma) \text{ with } \mu = \frac{\mu'}{\log_{10}(e)} \text{ and } \sigma = \frac{\sigma'}{\log_{10}(e)} \quad (4)$$

BA is therefore lognormally distributed with mean μ_{BA} and standard deviation σ_{BA} given by:

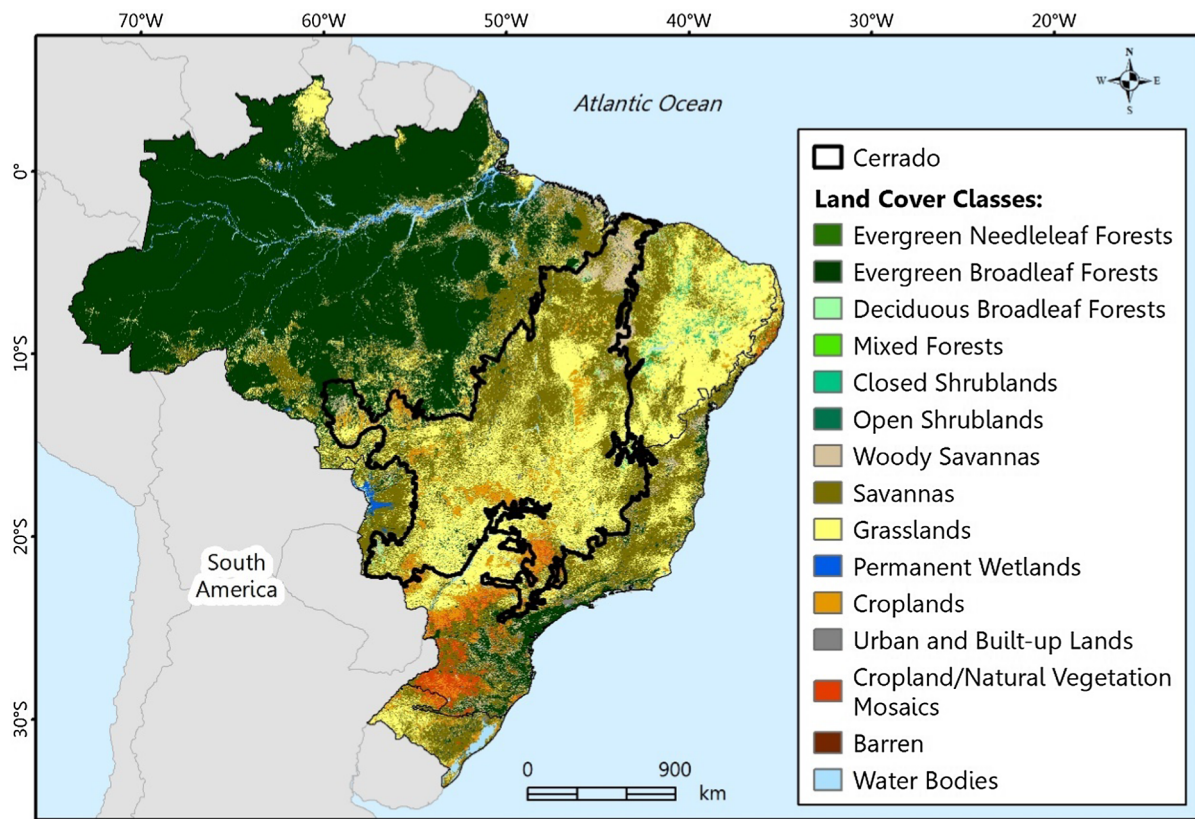


Fig. 1. Brazilian landcovers according to the International Geosphere-Biosphere Programme's classification scheme from the MCD12C1 product (Sulla-Menashe and Friedl, 2018). The thick black line delimits the Cerrado biome as defined by the Brazilian Institute of Environment and Renewable Natural Resources (IBAMA).

$$\mu_{BA} = e^{\mu + \frac{1}{2}\sigma^2} \text{ and } \sigma_{BA} = \sqrt{e^{2\mu + \sigma^2}(e^{\sigma^2} - 1)} \quad (5)$$

Finally, a unilateral test for differences of mean under independence was employed to account for the significance of future results (Wilks, 2011).

3. Results and discussion

3.1. Observation-based data

The annual cycles of DSR and of BA for the period 2003–2017 are shown in Fig. 2. There is a pronounced maximum of DSR in austral winter (in August–September), followed by a steep decline during spring. The highest values of fire danger are given by MERRA-2 and the lowest by JRA-55. All reanalyses agree in the peaks in DSR and show similar variations throughout the year. Results corroborate those of Carmona-Moreno et al. (2005), where the fire season in central Brazil is estimated from June to November. As with DSR, the highest values of BA occur in August and September. However, for all observation-derived DSR, a delay is seen as the peak of fire danger occurs in August whereas the peak of BA is in September. This might be due to vegetation accumulating stress in the highest fire danger months (i.e., with hottest and driest conditions) and therefore being more prone to burn afterward.

Changes in DSR from the three reanalyses might be traced back to differences between their annual cycles of the meteorological parameters in Cerrado (Fig. 3). Estimates of T are very similar throughout all reanalysis products, and the main differences are found between June and November where MERRA-2 tends to be warmer compared to ERA-I and JRA-55, both reaching about the same temperature in that period. This behaviour is in agreement with results by Auger et al. (2018), showing that, out of the three reanalyses, MERRA-2 achieves higher temperature over a considerable area of Cerrado and JRA-55 shows

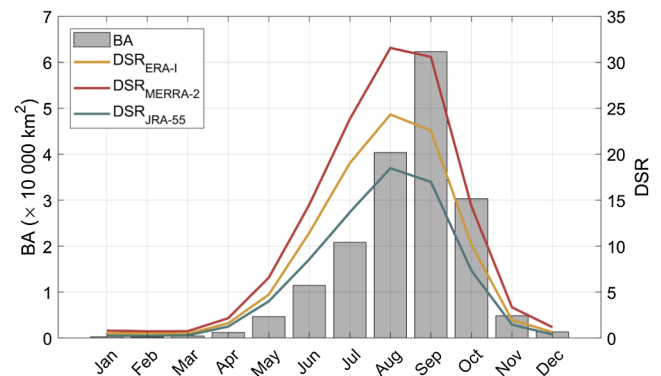


Fig. 2. Annual cycles of mean DSR (solid curves) and BA (bars) during the period 2003–2017. Annual cycles of DSR are derived from ERA-I (DSR_{ERA-I} ; yellow curve), MERRA-2 ($DSR_{MERRA-2}$; red curve) and JRA-55 (DSR_{JRA-55} ; green curve). The annual cycle of BA (grey bars) is based on the AQM product. (For interpretation of the references to colour in this figure legend, the reader is referred to the web version of this article.)

better agreement with T values from land surface stations.

As for RH, MERRA-2 shows considerably lower values than ERA-I and JRA-55. Both the above-mentioned higher T and lower RH explain the increased values of $DSR_{MERRA-2}$ when compared to the remaining reanalyses. Nonetheless, to test the weight of these meteorological parameters on DSR, MERRA-2 values of RH were incremented by 8% (as to approximate the estimates of ERA-I): the resulting DSR has a similar seasonal cycle to that of ERA-I, pointing to relative humidity as the main contributor to the increased DSR.

As expected, the annual cycle of BA is closely related to that of precipitation: fires are mainly observed throughout the dry season, between May and October, peaking in September and October during

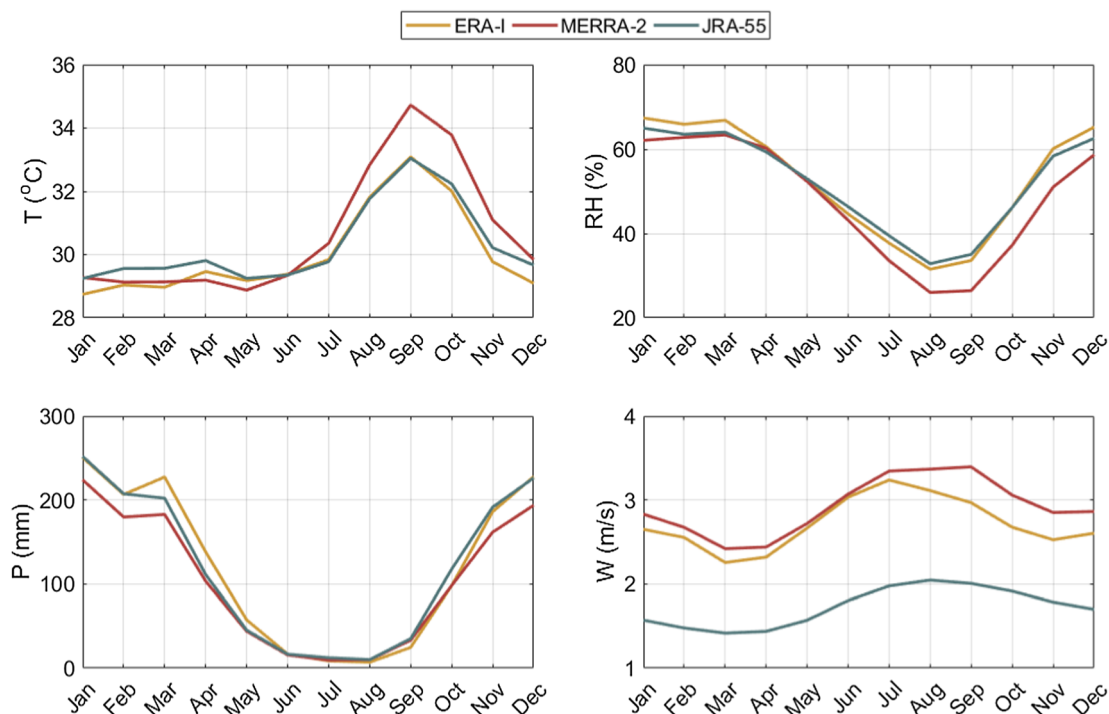


Fig. 3. Annual cycles of T, RH, P and W during the period 2003–2017 as derived from ERA-I (yellow curve), MERRA-2 (red curve) and JRA-55 (green curve) reanalyses. (For interpretation of the references to colour in this figure legend, the reader is referred to the web version of this article.)

the transition from dry to the rainy season. The peak of BA in the transition between the dry to rainy seasons in *Cerrado* regions has already been pointed out (Alvarado et al., 2017; Fornazari et al., 2015). In turn, early fires during the transition from rainy to dry season tend to be less severe given the higher moisture levels of accumulated fuel (Ramos-Neto and Pivello, 2000). Results shown in Fig. 3 agree with findings of Libonati et al. (2015), who obtained a correlation of 82% between burned area and precipitation. When compared to ERA-I, MERRA-2 presents a pronounced drier pattern over *Cerrado*, and in accordance with Lorenz and Kunstmann (2012) and Auger et al. (2018), it shows the lowest correlation with in situ measurements and global station data, whereas ERA-I shows slightly higher P rates when compared to ground observation, particularly from March to May and September to December.

Lastly, W presents the largest bias in observation-based estimations: values from JRA-55 are considerably lower than from ERA-I and MERRA-2. According to Torralba, Doblas-Reyes and Gonzalez-Reviriego (2017), compared to ERA-I and MERRA-2 the Japanese reanalysis provides lower values of W at the surface, probably due to the lowermost atmospheric level, where land surface processes occur, being placed too high over regions with trees. This is likely to be the reason to the lower values of DSR_{JRA-55} over the Brazilian *Cerrado*.

Fig. 4 shows the interannual variability of annual (grey bars) and fire season (dark grey portions) amounts of BA along with the observation-based DSR values throughout 2003–2017. On average, BA from August to October (defined here as the fire season) accounts for more than 3/5 of the annual amount.

All reanalyses present similar interannual variability with, as expected from previous results, DSR calculated from ERA-I showing intermediate values between those estimated from MERRA-2 and JRA-55. The interannual variability of BA in the fire season correlates well with the interannual variability of mean DSR. However, for all observation-based products, DSR also shows high values in 2015 and 2017 that present close to average values of BA. These variations of BA that are not reflected in changes of DSR, might be due to limitations of DSR, an index that is only determined by meteorological parameters and does

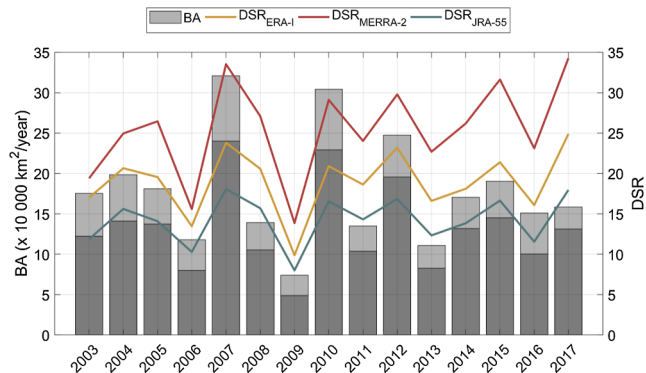


Fig. 4. Interannual variability during the period 2003–2017, of the accumulated values over the fire season (August to October) of BA (grey bars) and DSR as derived from ERA-I (yellow curve), MERRA-2 (red curve) and JRA-55 (green curve) reanalyses. The dark grey portion of the bars indicates the contribution of BA during the fire season to the total amount. (For interpretation of the references to colour in this figure legend, the reader is referred to the web version of this article.)

not take into account anthropogenic activity. The latter that has been found to strongly influence fire in South America, namely by changing land use practices and providing ignition sources (Aldersley et al., 2011).

3.2. Burned area statistical models

Results obtained in the previous section suggest modelling burned area in *Cerrado* using DSR as predictor. Accordingly, a linear model was developed where mean DSR_{ERA-I} during the fire season is used as a predictor of the decimal logarithm of BA during the same period as derived from the AQM product. The selection of DSR_{ERA-I} was motivated by the fact that DSR_{ERA-I} presents intermediate values between those of $DSR_{MERRA-2}$ and DSR_{JRA-55} . The model has a coefficient of determination of 0.71 (p-value < 0.0001), therefore explaining a large

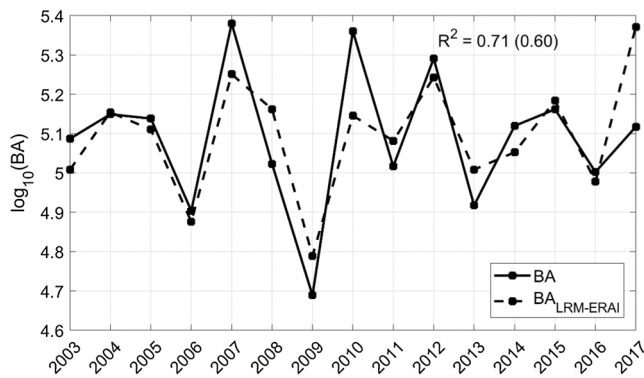


Fig. 5. Comparison of modelled BA by the linear regression model ($BA_{LRM-ERA-I}$) using mean DSR_{ERA-I} as a predictor, with observed BA derived from the AQM product.

part of the observation-based variability. The corresponding regression coefficient and intercept are, respectively, $m = 0.038$ and $b = 4.37$. After cross-validation the coefficient of determination shows a moderate decrease to 0.60, an indication of robustness of the fitted model (Fig. 5). A model of similar performance ($R^2 = 0.70$, p -value < 0.001) was obtained when using values of BA from MCD64 product, further confirming a strong and significant correlation.

Moreover, using the Monte Carlo approach, these strong relationships were proven to not arise by chance from a small sample of 15 independent values given that the 10 000 generated coefficients of determination obtained for the DSR_{ERA-I} and BA linear correlation are below the 99.9 percentile.

Results obtained for *Cerrado* confirm once again the versatility of the FWI system in replicating fire conditions throughout the globe. They further cement the role of climate in fire activity as the DSR, a solely climate-driven fire danger index, is able to accurately describe more than 2/3 of burned area in the Brazilian savanna. Given that fire ultimately depends on ignition, and as mentioned in previous sections, the remaining variability is likely to be attributed to anthropogenic activity mainly associated with land-use practices. Therefore, we hypothesize burned area can be fairly described and projected into the future by using only four climate variables: temperature, relative humidity, wind and precipitation. It is worth emphasizing the threefold role of temperature in fire dynamics (Flannigan et al., 2013): with increasing temperature, evapotranspiration increases as well and, as the ability for the atmosphere to hold moisture increases rapidly with higher temperatures, fuel moisture will decrease (unless there are significant increases in precipitation); with warmer temperatures there may be more lightning activity, which leads to increased natural ignitions; lastly, higher temperatures may lead to a lengthening of the fire season. In turn, wind is a strong component of fire behaviour, influencing its rate and direction of spread. It also supplies oxygen for the combustion process and reduces fuel moisture by increasing evaporation. Relative humidity reflects the amount of moisture that is in the atmosphere, which will affect the amount of moisture that is in the fuel and therefore its flammability. Lastly, precipitation is an essential factor in primary productivity, which has already been shown to be closely linked to fire activity (Bradstock, 2010; Paulucci et al., 2017; Pausas and Ribeiro, 2013). In intermediate-productivity environments, which is the case for Brazilian savannas, and in accordance with our results, sufficiently intense wet and dry seasons are needed to sustain high fire activity (Bowman et al., 2014).

3.3. Simulated climate

Using the same approach as for the reanalyses, the annual cycles of mean DSR calculated from RCA4 outputs (DSR_{RCA4}) were computed for the historical period (1976–2005) and for the three climate scenarios

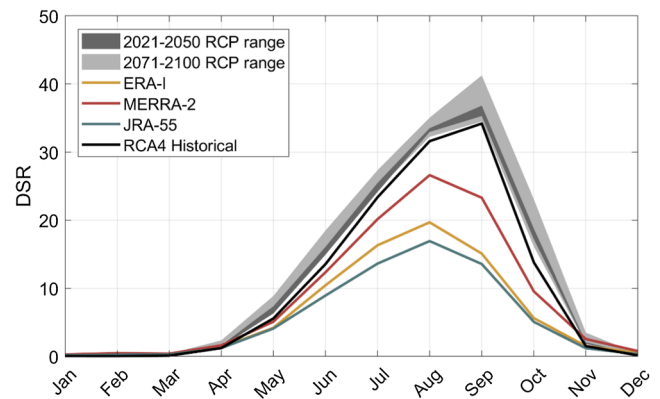


Fig. 6. Annual cycles of mean DSR_{RCA4} for the historical period (1976–2005) (solid thick black curves), and ranges of future changes using RCPs 2.6, 4.5 and 8.5 for the first (2021–2050, dark grey area) and second (2071–2100, light grey area) periods of the 21st century. The annual cycles of observation-based DSR are also provided for reference, as derived from ERA-I (yellow curve), MERRA-2 (red curve) and JRA-55 (green curve) for 1981–2005. (For interpretation of the references to colour in this figure legend, the reader is referred to the web version of this article.)

(RCPs 2.6, 4.5 and 8.5) in the first (2021–2050) and in the second (2071–2100) periods of the 21st century (Fig. 6). The annual cycles of the observation-based DSR (from ERA-I, MERRA-2, and JRA-55 reanalyses) for the period 1981–2005 are also shown for reference, indicating the uncertainty of observed climate.

Like the reanalyses, simulated data have annual cycles with a marked peak in winter. However, the peaks in the annual cycles of DSR_{RCA4} occur in September, whereas the peaks in the DSR cycles estimated by the reanalyses take place one month earlier, in August. This discrepancy is partially mitigated when aggregating DSR over the fire season (August to October). Moreover, as pointed out in Pereira et al. (2013), DSR is specifically appropriate to be averaged either in space and in time, an important feature since our study will deal with averaged fields of DSR performed over *Cerrado* and for the fire season.

The annual cycles of DSR_{RCA4} for future climate scenarios are systematically higher than the annual cycle of DSR for the historical period, the departures being especially larger during the fire season. In 2021–2050 the annual cycles of DSR_{RCA4} for all RCPs are very close to each other, presenting larger values of DSR than the annual cycle for the historical period in all months. In 2071–2100, there is a slight increase for RCP 4.5 and a large systematic positive change for RCP 8.5. This is not the case in scenario RCP 2.6, where there is a small decrease in DSR between 2021 and 2050 and 2071–2100. This is expected as RCP 2.6 is the only IPCC scenario in which the radiative forcing stabilizes mid-century onwards, reflected in the climate variables and thus DSR.

Systematic changes in the annual cycles of DSR_{RCA4} for the historical period and the future climate scenarios reflect changes in the annual cycles of T, RH, W and P (Fig. 7). For instance, the values of simulated RH and T in the dry season are lower than those of the reanalyses, and the lower values of simulated P also persist until September, suggesting an extended dry season. Since the resulting DSR values are higher than the observation-based data (Fig. 6), we hypothesize that the fire danger index in *Cerrado* is less sensitive to thermal conditions than to moisture and rainfall. This was further confirmed by considering the two periods of future climate scenarios (2021–2050 and 2071–2100) and evaluating the linear correlation between fire season averaged DSR_{RCA4} and corresponding averages of each meteorological parameter. Correlations for all periods and scenarios are statistically significant (p -value < 0.05) and it is worth mentioning that RH explains more than 80% of the interannual variability of DSR_{RCA4} , followed by P explaining more than 50%.

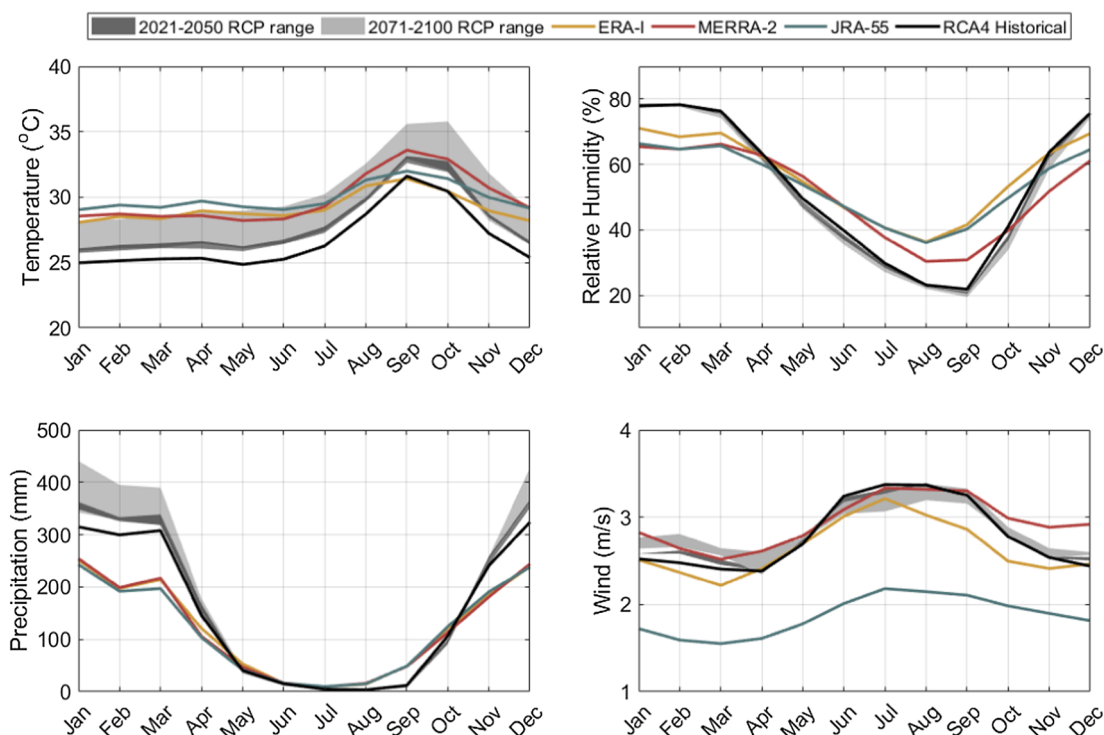


Fig. 7. Annual cycles of simulated T, RH, P and W, as derived from RCA4 for the historical period (1976–2005) (black curves) and ranges of simulated future changes using RCPs 2.6, 4.5 and 8.5 for 2021–2050 (dark grey area) and 2071–2100 (light grey area). The annual cycles of observation-based meteorological parameters are also provided for reference, as derived from ERA-I (yellow curve), MERRA-2 (red curve) and JRA-55 (green curve) for the 1981–2005 period. (For interpretation of the references to colour in this figure legend, the reader is referred to the web version of this article.)

In 2021–2050 all RCPs present similar annual cycles that have systematically lower (higher) values of RH (T) than those of the cycles in the historical period, and in 2071–2100 a decrease (increase) relative to 2021–2050 is observed for RCP 8.5. In the case of precipitation, virtually no changes are observed from May to October; changes in DSR_{RCA4} during the fire season between the historical period and the future scenarios (Fig. 6) are therefore determined by changes in T, RH, and W. However, for all scenarios, there is an increase of P from December to March compared to the historical period, an interesting feature because such strong changes in the precipitation cycle may alter the characteristics of vegetation cover and indirectly change the meteorological fire danger. Higher rainfall in the growing season (defined from October to April in Alvarado *et al.* [2017]) could lead to higher amounts of available biomass. On the other hand, higher precipitation in the transition from wet to dry season suggests higher soil moisture which could also lead to decreased fire risk.

3.4. Future projections of burned area

The BAM developed in Section 3.2 are then used to estimate future BA based on changes in DSR. For this purpose, normal distributions were fitted to the sample of DSR_{ERA-I} for the period 1981–2005 that were used in the BAM as well as to the samples of DSR_{RCA4} during the same period. Using the Lilliefors test the null hypothesis of normality is accepted for samples of both DSR_{ERA-I} and DSR_{RCA4} at the 5% significance level.

Samples of DSR_{RCA4} are then corrected so that the normal fitted distributions have the same mean and standard deviation of the corresponding distributions of DSR_{ERA-I} . Normal distributions were then fitted to values of DSR_{RCA4} for the 30-year historical period (1976–2005) and for the two 30-year periods of the 21st century (2021–2050 and 2071–2100) of the three RCPs. The null hypothesis of normality is accepted at the 5% significance level for all periods and scenarios. All samples of DSR_{RCA4} were then corrected using the

transformation that was used to convert the simulation-based normal distribution into the observation-based one in the validation period of 1981–2005 (Table 1).

Samples of BA for all scenarios and periods were then generated by applying the BAM to the corrected sample of DSR_{RCA4} ($DSR_{RCA4,corr}$). Since the BAM is linear and the distributions of $DSR_{RCA4,corr}$ are normal, obtained samples of the decimal logarithm of BA also have normal distributions and may be characterized by their means and standard deviations. As such, BA presents a lognormal distribution and its mean and standard deviation may be estimated using (5) as described in Section 2.6.

In all scenarios, an increase compared to historical BA is to be expected from the changes in DSR (Fig. 8, Table 2). This is in accordance with previous studies projecting an increased likelihood of large fire events throughout the 21st century (Flannigan *et al.*, 2013; Liu *et al.*, 2010; Silva *et al.*, 2016).

Nevertheless, important differences are found between the different scenarios: RCP 2.6 leads to an increase in the mean BA by mid-21st

Table 1
Mean, standard deviation and p-values from the unilateral test, of corrected fire season averaged DSR_{RCA4} for the historical period and future scenarios. Means of future scenarios that are significantly greater than the mean for the historical period at the 5% significance level are highlighted in bold.

		Mean	St. dev	p-value
Historical	1976–2005	13.58	3.78	
RCP 2.6	2021–2050	15.83	3.72	0.01
	2071–2100	14.83	3.64	0.1
RCP 4.5	2021–2050	17.08	4.35	4×10^{-4}
	2071–2100	17.05	4.61	7×10^{-4}
RCP 8.5	2021–2050	16.86	3.68	3×10^{-4}
	2071–2100	21.11	4.16	1×10^{-13}

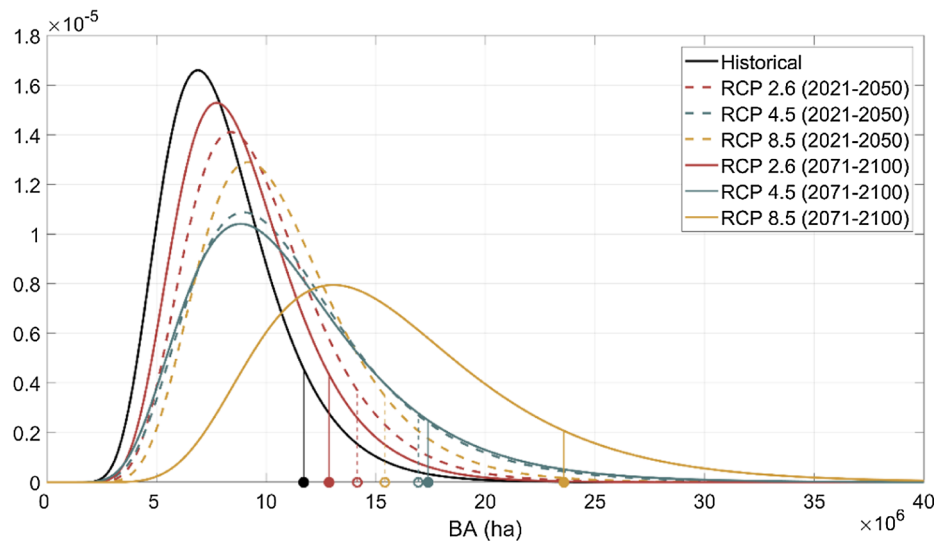


Fig. 8. Lognormal distributions of BA (in 10^6 ha) as estimated from the BAM using DSR_{RCA4_corr} as predictor for the historical period (1976–2005; solid black curve) and for the 2021–2050 (dashed coloured curves) and 2071–2100 (solid coloured curves) periods of RCP 2.6 (red), RCP 4.5 (green) and RCP 8.5 (yellow). Circles in the x-axis indicate values of percentile 90 of each curve. (For interpretation of the references to colour in this figure legend, the reader is referred to the web version of this article.)

century followed by a reduction by the end of the century (linked to a decrease in radiative forcing by the century compared to mid-century estimates). Under this scenario, BA also becomes less variable. RCP 4.5 and 8.5 scenarios lead to similar increases in mean BA by mid-21st century, consistent with similar pathways up to 2050 (IPCC, 2013). Differences between these two values (respectively 17.08 for RCP 4.5 and 16.86 for RCP 8.5) are not noteworthy taking into account the respective values of the standard deviations (4.35 for RCP 4.5 and 3.68 for RCP 8.5). RCP 8.5 leads to an increase 4×10^6 ha higher than RCP 4.5 and almost 7×10^6 ha higher than RCP 2.6. Moreover, both scenarios are also characterized by an increase in standard deviation of BA, associated with increased probability of occurrence of extreme fire seasons.

The only scenario which did not pass the unilateral test was RCP 2.6 in the 2071–2100 period, showing no significant changes from the historical period (Table 2). These results take special relevance given that scenario RCP 2.6 is comparable to the 1.5 °C warming relative to the pre-industrial period by the end of the century goal established by the United Nations. Differences in future BA in the Brazilian *Cerrado* between RCP 2.6 and both RCP 4.5 and 8.5 are considerable, especially regarding extreme events. The percentiles 90 of RCP 4.5 and 8.5 for both periods are considerably higher than RCP 2.6, especially by the end of the century. Extreme BA events will thus be more frequent in the intermediate and severe climate scenarios, compared to RCP 2.6. In the latter, percentile 90 peaks by mid-century to then decrease, meaning that extreme events will also be reduced following the peak, contrasting with the remaining scenarios. RCP 2.6 reaches the most similar values

Table 2

As in Table 1, but for mean, standard deviation and percentile 90 of estimated BA (expressed in units of 10^6 ha).

		Mean	St. dev	P ₉₀	p-value
Historical	1976–2005	8.11	2.75	11.72	
RCP 2.6	2021–2050	9.85	3.28	14.16	0.01
	2071–2100	9.01	2.94	12.87	0.1
RCP 4.5	2021–2050	11.20	4.41	16.95	6×10^{-4}
	2071–2100	11.27	4.72	17.40	8×10^{-4}
RCP 8.5	2021–2050	10.76	3.55	15.42	6×10^{-4}
	2071–2100	15.82	5.94	23.58	6×10^{-11}

to that of historical BA, further confirming the importance of aiming for the 1.5 °C target.

For the intermediate scenario, most of the changes will occur in the first half of the century, a result in accordance with those from van Vuuren et al. (2011) who estimated a decrease/stabilization of GHG and radiative forcing after 2050 for this scenario. On the other hand, RCP 8.5 shows major increases in the mean and standard deviation of the future BA by the end of the century when compared to historical values and other scenarios. This outcome, however, is likely not realistic, since only meteorological factors were taken into account in the analysis and the interactions between vegetation and fire were not considered.

It is well known that fires result from several interacting factors, namely climate, fuels, ignitions, land cover type and land use, which change through time. Recent studies have found a global BA decline due to anthropogenic influence (Andela et al., 2017; Li et al., 2018); a substantial portion of native vegetation was cleared, mostly for agricultural purposes, and turned into grasslands and croplands where fire does not reach considerable dimensions (Strassburg et al., 2017). Regarding Brazil, a decrease in burned area has been found in the southwest part of *Cerrado*, but the northeast shows an increase in BA in the past decade. The latter region is the new agricultural frontier whereas the former has mostly been cleared of native vegetation and is now dominated by grasslands and croplands (Françoso et al., 2015; Zalles et al., 2019). Therefore, even if climate has a prominent role in fire occurrence explaining about two thirds of the interannual variability of BA in *Cerrado*, the role of human activity has also to be considered when analysing our results for present and future climate. It is also worth noting that, RCPs do consider distinct future anthropogenic land-use practices (van Vuuren et al., 2011); both RCP 2.6 and 8.5 estimate increased cropland/grassland area which might indicate that more native vegetation will be cleared, whereas RCP 4.5 entails that native vegetation will be regained.

4. Conclusions

We developed a statistical model to estimate BA in the Brazilian *Cerrado* using DSR as a proxy of climate conditions. The model explains 71% of the interannual variability of BA for the period 2003–2017, therefore raising the prospect to apply it to future climate projections in *Cerrado*. This was achieved by feeding the statistical model with DSR

computed using simulated meteorological fields from a regional climate model (RCA4) for three future climate scenarios (RCP 2.6, 4.5 and 8.5).

Our results indicate that, in all climate scenarios, changes in the distributions of BA in *Cerrado* are to be expected along the 21st century, in terms of mean, variability and frequency of extreme events. In the case of RCP 4.5 and 8.5, a systematic increase is found in the mean, the standard deviation and percentile 90 of distributions of BA from the historical period (1976–2005) to 2021–2050 up to 2071–2100. In the case of RCP 2.6 the mean, the standard deviation and percentile 90, all decrease from 2021–2050 to 2071–2100, therefore highlighting the importance of the ambitious greenhouse gas emissions reduction policies associated to the mildest scenario.

Given the flexibility of the proposed approach, results here obtained at the biome level can be refined by applying it to subregions of similar fire regime and/or climate types in *Cerrado*. Regarding the short period covered by the currently available satellite-based burned area dataset, this limitation was partially circumvented by comparing recent past distributions of observation-based fields with simulated outputs for the historical period. Lastly, as in the case of reanalyses, where three different datasets were used to provide a measure of uncertainty, a similar approach could be applied using outputs from other RCMs when they become available for South America.

Results from this work emphasize the importance of limiting warming to 1.5 °C by the end of the century in order to minimize the environmental and social costs associated with fires. Increased fire activity and limited regeneration can significantly contribute to increased concentrations of carbon in the atmosphere, as not only fires themselves release carbon but they also decimate forest which would consume it. Ending ecosystem degradation and disturbance could reduce emissions by 862 TgC/yr, possibly paving a path for a low-emission future (Baccini et al., 2017). Any further warming will strongly amplify fire danger and lead to strong increases in BA in *Cerrado*, which may lead to major economic and environmental losses and to a considerable growth in spending in fire mitigation. Furthermore, increasingly frequent extreme events such as heat waves (Geirinhas et al., 2018; Perkins et al., 2012; Rusticucci, 2012) and droughts (Marengo and Espinoza, 2016; Panisset et al., 2018), can potentially aggravate fire events by increasing the probability of occurrence of high severity episodes. In fact, according to several studies, Brazil is expected to become drier (Duffy et al., 2015; Guimberteau et al., 2013; Marengo et al., 2012) and warmer (Moritz et al., 2012), affecting ecosystems and promoting conditions for fire activity (Le Page et al., 2017; Silva et al., 2016).

As a fire-dependent biome, *Cerrado* may recover and adapt more easily to higher fire danger, and increased fire activity, than fire-sensitive biomes. Nevertheless, high severity fires and vast burned areas can still irreparably damage fire-prone ecosystems. Therefore, we argue that current Brazilian policies will be crucial in determining how severe fires will be in *Cerrado* for the future.

Declaration of Competing Interest

None.

Acknowledgements

This work was developed within the framework of the Brazilian Fire-Land-Atmosphere System (BrFLAS) Project financed by the Portuguese and Brazilian science foundations, FCT and FAPESP (project references FAPESP/1389/2014 and 2014/20042-2). RL was funded by Serrapilheira Institute (grant number Serra-1708-15159) and by CNPQ (441971/2018-0 and 305159/2018-6).

Appendix A. Supplementary material

Supplementary data to this article can be found online at <https://doi.org/10.1016/j.foreco.2019.05.047>.

References

- Aldersley, A., Murray, S.J., Cornell, S.E., 2011. Global and regional analysis of climate and human drivers of wildfire. *Sci. Total Environ.* 409, 3472–3481. <https://doi.org/10.1016/j.scitotenv.2011.05.032>.
- Alvarado, S.T., Fornazari, T., Cóstola, A., Morellato, L.P.C., Silva, T.S.F., 2017. Drivers of fire occurrence in a mountainous Brazilian *Cerrado* savanna: Tracking long-term fire regimes using remote sensing. *Ecol. Ind.* 78, 270–281. <https://doi.org/10.1016/j.ecolind.2017.02.037>.
- Andela, N., Morton, D.C., Giglio, L., Chen, Y., van der Werf, G.R., Kasibhatla, P.S., DeFries, R.S., Collatz, G.J., Hantson, S., Kloster, S., Bachelet, D., Forrest, M., Lasslop, G., Li, F., Mangeon, S., Melton, J.R., Yue, C., Randerson, J.T., 2017. A human-driven decline in global burned area. *Science* 356, 1356–1362. <https://doi.org/10.1126/science.aal4108>.
- Auger, J., Birkel, S., Maasch, K., Mayewski, P., Schuenemann, K., Auger, J.D., Birkel, S.D., Maasch, K.A., Mayewski, P.A., Schuenemann, K.C., 2018. An ensemble mean and evaluation of third generation global climate reanalysis models. *Atmosphere* (Basel). 9, 236. <https://doi.org/10.3390/atmos9060236>.
- Baccini, A., Walker, W., Carvalho, L., Farina, M., Sulla-Menashe, D., Houghton, R.A., 2017. Tropical forests are a net carbon source based on aboveground measurements of gain and loss. *Science* (80-) 358, 230–234. <https://doi.org/10.1126/science.aam5962>.
- Bond, W., Keeley, J., 2005. Fire as a global 'herbivore': the ecology and evolution of flammable ecosystems. *Trends Ecol. Evol.* 20, 387–394. <https://doi.org/10.1016/j.tree.2005.04.025>.
- Bosilovich, M.G., Chen, J., Robertson, F.R., Adler, R.F., 2008. Evaluation of global precipitation in reanalyses. *J. Appl. Meteorol. Climatol.* 47, 2279–2299. <https://doi.org/10.1175/2008JAMC1921.1>.
- Bowman, D.M.J.S., Balch, J.K., Artaxo, P., Bond, W.J., Carlson, J.M., Cochrane, M.A., D'Antonio, C.M., DeFries, R.S., Doyle, J.C., Harrison, S.P., Johnston, F.H., Keeley, J.E., Krawchuk, M.A., Kull, C.A., Marston, J.B., Moritz, M.A., Prentice, I.C., Roos, C.I., Scott, A.C., Swetnam, T.W., van der Werf, G.R., Pyne, S.J., 2009. Fire in the earth system. *Science* (80-) 324. <https://doi.org/10.1126/science.1163886>.
- Bowman, D.M.J.S., Murphy, B.P., Williamson, G.J., Cochrane, M.A., 2014. Pyrogeographic models, feedbacks and the future of global fire regimes. *Glob. Ecol. Biogeogr.* 23, 821–824. <https://doi.org/10.1111/geb.12180>.
- Bradstock, R.A., 2010. A biogeographic model of fire regimes in Australia: current and future implications. *Glob. Ecol. Biogeogr.* 19, 145–158. <https://doi.org/10.1111/j.1466-8238.2009.00512.x>.
- Brunke, M.A., Wang, Z., Zeng, X., Bosilovich, M., Shie, C.-L., 2011. An assessment of the uncertainties in ocean surface turbulent fluxes in 11 reanalysis, satellite-derived, and combined global datasets. *J. Clim.* 24, 5469–5493. <https://doi.org/10.1175/2011JCLI4223.1>.
- Carmona-Moreno, C., Belward, A., Malingreau, J.-P., Hartley, A., Garcia-Alegre, M., Antonovskiy, M., Buchshtaber, V., Pivovarov, V., 2005. Characterizing interannual variations in global fire calendar using data from Earth observing satellites. *Glob. Chang. Biol.* 11, 1537–1555. <https://doi.org/10.1111/j.1365-2486.2005.01003.x>.
- Carvalho, A.C., Carvalho, A., Martins, H., Marques, C., Rocha, A., Borrego, C., Viegas, D.X., Miranda, A.I., 2011. Fire weather risk assessment under climate change using a dynamical downscaling approach. *Environ. Model. Softw.* 26, 1123–1133. <https://doi.org/10.1016/j.envsoft.2011.03.012>.
- Chen, Y., Randerson, J.T., Morton, D.C., DeFries, R.S., Collatz, G.J., Kasibhatla, P.S., Giglio, L., Jin, Y., Marlier, M.E., 2011. Forecasting fire season severity in South America using sea surface temperature anomalies. *Science* 334, 787–791. <https://doi.org/10.1126/science.1209472>.
- Chuvieco, E., Yue, C., Heil, A., Mouillot, F., Alonso-Canas, I., Padilla, M., Pereira, J.M., Oom, D., Tansey, K., 2016. A new global burned area product for climate assessment of fire impacts. *Glob. Ecol. Biogeogr.* 25, 619–629. <https://doi.org/10.1111/geb.12440>.
- DaCamara, C.C., Libonati, R., Ermida, S.L., Calado, T.J., 2016. A user-oriented simplification of the (V, W) burn-sensitive vegetation index system. *IEEE Geosci. Remote Sens. Lett.* 13, 1822–1826. <https://doi.org/10.1109/LGRS.2016.2614319>.
- Dantas, V.de.L., Batalha, M.A., Pausas, J.G., 2013a. Fire drives functional thresholds on the savanna-forest transition. *Ecology* 94, 2454–2463. <https://doi.org/10.1890/12-1629.1>.
- Dantas, V.de.L., Pausas, J.G., Batalha, M.A., de Paula Lioioli, P., Cianciaruso, M.V., 2013b. The role of fire in structuring trait variability in Neotropical savannas. *Oecologia* 171, 487–494. <https://doi.org/10.1007/s00442-012-2431-8>.
- DeBano, L.F., Neary, D.G., Ffolliott, P.F., 1998. *Fire's Effects on Ecosystems*. J. Wiley.
- Dee, D.P., Uppala, S.M., Simmons, A.J., Berrisford, P., Poli, P., Kobayashi, S., Andrae, U., Balmasada, M.A., Balsamo, G., Bauer, P., Bechtold, P., Beljaars, A.C.M., van de Berg, L., Bidlot, J., Bormann, N., Delsol, C., Dragani, R., Fuentes, M., Geer, A.J., Haimberger, L., Healy, S.B., Hersbach, H., Hólm, E.V., Isaksen, I., Kållberg, P., Köhler, M., Matricardi, M., McNally, A.P., Monge-Sanz, B.M., Morcrette, J.-J., Park, B.-K., Peubey, C., de Rosnay, P., Tavolato, C., Thépaut, J.-N., Vitart, F., 2011. The ERA-Interim reanalysis: configuration and performance of the data assimilation system. *Q. J. R. Meteorol. Soc.* 137, 553–597. <https://doi.org/10.1002/qj.828>.
- Dietrich, C., Schimanke, S., Wang, S., Väli, G., Liu, Y., Horndorff, R., Axell, L., Höglund, A., Meier, H.E., 2013. Evaluation of the SMHI coupled atmosphere-ice-ocean model RCA4-NEMO.
- Duffy, P.B., Brando, P., Asner, G.P., Field, C.B., 2015. Projections of future meteorological drought and wet periods in the Amazon. *Proc. Natl. Acad. Sci. U. S. A.* 112, 13172–13177. <https://doi.org/10.1073/pnas.1421011112>.
- Durigan, G., Ratter, J.A., 2016. The need for a consistent fire policy for *Cerrado* conservation. *J. Appl. Ecol.* 53, 11–15. <https://doi.org/10.1111/1365-2664.12559>.

- Durigan, G., de Siqueira, M.F., Franco, G.A.D.C., 2007. Threats to the Cerrado remnants of the state of São Paulo, Brazil. *Sci. Agric.* 64, 355–363. <https://doi.org/10.1590/S0103-90162007000400006>.
- Falco, M., Carril, A.F., Menéndez, C.G., Zaninelli, P.G., Li, L.Z.X., 2018. Assessment of CORDEX simulations over South America: added value on seasonal climatology and resolution considerations. *Clim. Dyn.* 1–16. <https://doi.org/10.1007/s00382-018-4412-z>.
- Fidelis, A., Alvarado, S., Barradas, A., Pivello, V., 2018. The Year 2017: Megafires and Management in the Cerrado. *Fire* 1, 49. <https://doi.org/10.3390/fire1030049>.
- Flannigan, M., Cantin, A.S., de Groot, W.J., Wotton, M., Newbery, A., Gowman, L.M., 2013. Global wildland fire season severity in the 21st century. *For. Ecol. Manage.* 294, 54–61. <https://doi.org/10.1016/J.FORECO.2012.10.022>.
- Fornazari, T., Freire, T.S., Swanni, S., Alvarado, T., Patrícia, L., Morellato, C., 2015. Variáveis limitantes sobre a detecção de queimadas em imagens Landsat no Parque Nacional da Serra do Cipó (MG).
- Françoso, R.D., Brandão, R., Nogueira, C.C., Salmona, Y.B., Machado, R.B., Colli, G.R., 2015. Habitat loss and the effectiveness of protected areas in the Cerrado Biodiversity Hotspot. *Nat. Conserv.* 13, 35–40. <https://doi.org/10.1016/J.NCON.2015.04.001>.
- Geirinhas, J.L., Trigo, R.M., Libonati, R., Coelho, C.A.S., Palmeira, A.C., 2018. Climatic and synoptic characterization of heat waves in Brazil. *Int. J. Climatol.* 38, 1760–1776. <https://doi.org/10.1002/joc.5294>.
- Gelaro, R., McCarty, W., Suárez, M.J., Todling, R., Molod, A., Takacs, L., Randles, C.A., Darmenov, A., Bosilovich, M.G., Reichle, R., Wargan, K., Coy, L., Cullather, R., Draper, C., Akella, S., Buchard, V., Conaty, A., da Silva, A.M., Gu, W., Kim, G.-K., Koster, R., Lucchesi, R., Merkova, D., Nielsen, J.E., Partyka, G., Pawson, S., Putman, W., Rienecker, M., Schubert, S.D., Sienkiewicz, M., Zhao, B., 2017. The modern-era retrospective analysis for research and applications, Version 2 (MERRA-2). *J. Clim.* 30, 5419–5454. <https://doi.org/10.1175/JCLI-D-16-0758.1>.
- Giglio, L., Boschetti, L., Roy, D.P., Humber, M.L., Justice, C.O., 2018. The collection 6 MODIS burned area mapping algorithm and product. *Remote Sens. Environ.* 217, 72–85. <https://doi.org/10.1016/J.RSE.2018.08.005>.
- Giglio, L., Schroeder, W., Justice, C.O., 2016. The collection 6 MODIS active fire detection algorithm and fire products. *Remote Sens. Environ.* 178, 31–41. <https://doi.org/10.1016/J.RSE.2016.02.054>.
- Gillett, N.P., Weaver, A.J., Zwiwers, F.W., Flannigan, M.D., 2004. Detecting the effect of climate change on Canadian forest fires. *Geophys. Res. Lett.* 31, L18211. <https://doi.org/10.1029/2004GL020876>.
- Giorgi, F., Jones, C., Asrar, G.R., 2009. Addressing climate information needs at the regional level: the CORDEX framework. *WMO Bulletin*.
- Gomes, L., Miranda, H.S., Bustamante, M.M.d.A.C., 2018. How can we advance the knowledge on the behavior and effects of fire in the Cerrado biome? *For. Ecol. Manage.* 417, 281–290. <https://doi.org/10.1016/J.FORECO.2018.02.032>.
- Gorgone-Barbosa, E., 2016. A relação entre fogo e uma gramínea invasora no Cerrado: O fogo pode ser utilizado, como uma estratégia de controle? Universidade Estadual Paulista “Júlio De Mesquita Filho.”
- Guimbertau, M., Ronchail, J., Espinoza, J.C., Lengaigne, M., Sultan, B., Polcher, J., Drapeau, G., Guyot, J.-L., Ducharne, A., Ciais, P., 2013. Future changes in precipitation and impacts on extreme streamflow over Amazonian sub-basins. *Environ. Res. Lett.* 8, 014035. <https://doi.org/10.1088/1748-9326/8/1/014035>.
- Hantson, S., Armeth, A., Harrison, S.P., Kelley, D.L., Colin Prentice, I., Rabin, S.S., Archibald, S., Mouillot, F., Arnold, S.R., Artaxo, P., Bachelet, D., Ciais, P., Forrest, M., Friedlingstein, P., Hickler, T., Kaplan, J.O., Kloster, S., Knorr, W., Lasslop, G., Li, F., Mangleon, S., Melton, J.R., Meyn, A., Sitch, S., Spessa, A., Van Der Werf, G.R., Voulgarakis, A., Yue, C., 2016. The status and challenge of global fire modelling. *Biogeosciences* 13, 3359–3375. <https://doi.org/10.5194/bg-13-3359-2016>.
- Hantson, S., Pueyo, S., Chuvieco, E., 2015. Global fire size distribution is driven by human impact and climate. *Glob. Ecol. Biogeogr.* 24, 77–86. <https://doi.org/10.1111/geb.12246>.
- Hardesty, J., Myers, R., Fulks, W., 2005. Fire, ecosystems and people: a preliminary assessment of fire as a global conservation issue. *Fire Manage.* 22, 78–87. <https://doi.org/10.1177/0146167209351886>.
- Hazeleger, W., Wang, X., Severijns, C., Ștefănescu, S., Bintanja, R., Sterl, A., Wyser, K., Semmler, T., Yang, S., van den Hurk, B., van Noije, T., van der Linden, E., van der Wiel, K., 2012. EC-Earth V2.2: description and validation of a new seamless earth system prediction model. *Clim. Dyn.* 39, 2611–2629. <https://doi.org/10.1007/s00382-011-1228-5>.
- Hoffmann, W.A., 1999. Fire and population dynamics of woody plants in a neotropical savanna: matrix model projections. *Ecology* 80, 1354–1369. [https://doi.org/10.1890/0012-9658\(1999\)080\[1354:FAPDOW\]2.0.CO;2](https://doi.org/10.1890/0012-9658(1999)080[1354:FAPDOW]2.0.CO;2).
- Hoffmann, W.A., Geiger, E.L., Gotsch, S.G., Rossatto, D.R., Silva, L.C.R., Lau, O.L., Haridasan, M., Franco, A.C., 2012a. Ecological thresholds at the savanna-forest boundary: how plant traits, resources and fire govern the distribution of tropical biomes. *Ecol. Lett.* 15, 759–768. <https://doi.org/10.1111/j.1461-0248.2012.01789.x>.
- Hoffmann, W.A., Jaconis, S.Y., Mckinley, K.L., Geiger, E.L., Gotsch, S.G., Franco, A.C., 2012b. Fuels or microclimate? Understanding the drivers of fire feedbacks at savanna-forest boundaries. *Austral Ecol.* 37, 634–643. <https://doi.org/10.1111/j.1442-9993.2011.02324.x>.
- IPCC, 2013. Climate Change 2013: The Physical Science Basis. In: Contribution of Working Group I to the Fifth Assessment Report of the Intergovernmental Panel on Climate Change. Cambridge University Press, Cambridge, United Kingdom and New York, NY, USA. <https://doi.org/10.1017/CBO9781107415324>.
- Iqbal, W., Syed, F.S., Sajjad, H., Nikulin, G., Kjellström, E., Hannachi, A., 2017. Mean climate and representation of jet streams in the CORDEX South Asia simulations by the regional climate model RCA4. *Theor. Appl. Climatol.* 129, 1–19. <https://doi.org/10.1007/s00704-016-1755-4>.
- Kim, H.-G., Kim, J.-Y., Kang, Y.-H., 2018. Comparative evaluation of the third-generation reanalysis data for wind resource assessment of the southwestern offshore in South Korea. *Atmosphere (Basel)* 9, 73. <https://doi.org/10.3390/atmos9020073>.
- Kloster, S., Lasslop, G., 2017. Historical and future fire occurrence (1850 to 2100) simulated in CMIP5 Earth System Models. *Glob. Planet. Change* 150, 58–69. <https://doi.org/10.1016/J.GLOPLACHA.2016.12.017>.
- Kobayashi, S., Ota, Y., Harada, Y., Ebata, A., Moriya, M., Onoda, H., Onogi, K., Kamahori, H., Kobayashi, C., Endo, H., Miyaoka, K., Takahashi, K., 2015. The JRA-55 reanalysis: general specifications and basic characteristics. *J. Meteorol. Soc. Japan. Ser. II* 93, 5–48. <https://doi.org/10.2151/jmsj.2015-001>.
- Kozłowski, T.T., Theodore, T., Ahlgren, C.E., Clifford E., 1974. Fire and ecosystems.
- Le Page, Y., Morton, D., Hartin, C., Bond-Lamberty, B., Pereira, J.M.C., Hurtt, G., Asrar, G., 2017. Synergy between land use and climate change increases future fire risk in Amazon forests. *Earth Syst. Dyn.* 8, 1237–1246. <https://doi.org/10.5194/esd-8-1237-2017>.
- Li, F., Lawrence, D.M., Bond-Lamberty, B., 2018. Human impacts on 20th century fire dynamics and implications for global carbon and water trajectories. *Glob. Planet. Change* 162, 18–27. <https://doi.org/10.1016/J.GLOPLACHA.2018.01.002>.
- Libonati, R., DaCamara, C., Setzer, A., Morelli, F., Melchiori, A., 2015. An algorithm for burned area detection in the Brazilian Cerrado using 4 μm MODIS imagery. *Remote Sens.* 7, 15782–15803. <https://doi.org/10.3390/rs71115782>.
- Libonati, R., DaCamara, C.C., Pereira, J.M.C., Peres, L.F., 2011. On a new coordinate system for improved discrimination of vegetation and burned areas using MIR/NIR information. *Remote Sens. Environ.* 115, 1464–1477. <https://doi.org/10.1016/J.RSE.2011.02.006>.
- Lilliefors, H.W., 1967. On the Kolmogorov-Smirnov test for normality with mean and variance unknown. *J. Am. Stat. Assoc.* 62, 399. <https://doi.org/10.2307/2283970>.
- Liu, Y., Stanturf, J., Goodrick, S., 2010. Trends in global wildfire potential in a changing climate. *For. Ecol. Manage.* 259, 685–697. <https://doi.org/10.1016/J.FORECO.2009.09.002>.
- Lorenz, C., Kunstmann, H., 2012. The hydrological cycle in three state-of-the-art re-analyses: intercomparison and performance analysis. *J. Hydrometeorol.* 13, 1397–1420. <https://doi.org/10.1175/JHM-D-11-088.1>.
- Marengo, J.A., Chou, S.C., Kay, G., Alves, L.M., Pesquero, J.F., Soares, W.R., Santos, D.C., Lyra, A.A., Sueiro, G., Betts, R., Chagas, D.J., Gomes, J.L., Bustamante, J.F., Tavares, P., 2012. Development of regional future climate change scenarios in South America using the Eta CPTEC/HadCM3 climate change projections: climatology and regional analyses for the Amazon, São Francisco and the Paraná River basins. *Clim. Dyn.* 38, 1829–1848. <https://doi.org/10.1007/s00382-011-1155-5>.
- Marengo, J.A., Espinoza, J.C., 2016. Extreme seasonal droughts and floods in Amazonia: causes, trends and impacts. *Int. J. Climatol.* 36, 1033–1050. <https://doi.org/10.1002/joc.4420>.
- Masson-Delmotte, V., Zhai, P., Pörtner, H.O., Roberts, D., Skea, J., Shukla, P.R., Pirani, A., Moufouma-Okia, W., Péan, C., Pidcock, R., Connors, S., Matthews, J.B.R., Chen, Y., Zhou, X., Gomis, M.L., Lonnoy, E., Maycock, T., Tignor, M., (eds.), T.W., 2018. IPCC, 2018: Summary for Policymakers. In: Global warming of 1.5°C. An IPCC Special Report on the impacts of global warming of 1.5°C above pre-industrial levels and related global greenhouse gas emission pathways, in the context of strengthening the global. Geneva, Switzerland.
- Menéndez, C.G., Giles, J., Ruscica, R., Zaninelli, P., Coronato, T., Falco, M., Sörensson, A., Fita, L., Carril, A., Li, L., 2019. Temperature variability and soil-atmosphere interaction in South America simulated by two regional climate models. *Clim. Dyn.* 1–12. <https://doi.org/10.1007/s00382-019-04668-6>.
- Miranda, H.S., Sato, M.N., Neto, W.N., Aires, F.S., 2009. Fires in the Cerrado, the Brazilian savanna. In: *Tropical Fire Ecology*. Springer Berlin Heidelberg, Berlin, Heidelberg, pp. 427–450. https://doi.org/10.1007/978-3-540-77381-8_15.
- Moritz, M.A., Parisien, M.-A., Batllori, E., Krawchuk, M.A., Van Dorn, J., Ganz, D.J., Hayhoe, K., 2012. Climate change and disruptions to global fire activity. <https://doi.org/10.1890/ES11-00345.1>.
- Myers, N., Mittermeier, R.A., Mittermeier, C.G., da Fonseca, G.A.B., Kent, J., 2000. Biodiversity hotspots for conservation priorities. *Nature* 403, 853–858. <https://doi.org/10.1038/35002501>.
- Nogueira, J., Rambal, S., Barbosa, J., Mouillot, F., 2017. Spatial pattern of the seasonal drought/burned area relationship across Brazilian biomes: sensitivity to drought metrics and global remote-sensing fire products. *Climate* 5, 42. <https://doi.org/10.3390/cli5020042>.
- Overbeck, G.E., Vélez-Martín, E., Scarano, F.R., Lewinsohn, T.M., Fonseca, C.R., Meyer, S.T., Müller, S.C., Ceotto, P., Dadalt, L., Durigan, G., Ganade, G., Gossner, M.M., Guadagnin, D.L., Lorenzen, K., Jacobi, C.M., Weisser, W.W., Pillar, V.D., 2015. Conservation in Brazil needs to include non-forest ecosystems. *Divers. Distrib.* 21, 1455–1460. <https://doi.org/10.1111/ddi.12380>.
- Panisset, J.S., Libonati, R., Gouveia, C.M.P., Machado-Silva, F., França, D.A., França, J.R.A., Peres, L.F., 2018. Contrasting patterns of the extreme drought episodes of 2005, 2010 and 2015 in the Amazon Basin. *Int. J. Climatol.* 38, 1096–1104. <https://doi.org/10.1002/joc.5224>.
- Paulucci, T.B., Machado-Silva, F., Libonati, R., 2017. Análise espaço-temporal da ocorrência de áreas queimadas no Cerrado para o período de 2005 a 2014 e sua relação com a precipitação. *An. do Simpósio Bras. Sensoriamento Remoto 2017 (33)*, 130–136.
- Pausas, J.G., Ribeiro, E., 2013. The global fire-productivity relationship. *Glob. Ecol. Biogeogr.* 22, 728–736. <https://doi.org/10.1111/geb.12043>.
- Pereira, M., Calado, T., DaCamara, C., Calheiros, T., 2013. Effects of regional climate change on rural fires in Portugal. *Clim. Res.* 57, 187–200. <https://doi.org/10.3354/cr01176>.
- Perkins, S.E., Alexander, L.V., Nairn, J.R., 2012. Increasing frequency, intensity and duration of observed global heatwaves and warm spells. *Geophys. Res. Lett.* 39,

20714. <https://doi.org/10.1029/2012GL053361>.
- Pinto, M.M., DaCamara, C.C., Trigo, I.F., Trigo, R.M., Turkman, K.F., 2018. Fire danger rating over Mediterranean Europe based on fire radiative power derived from Meteosat. *Nat. Hazards Earth Syst. Sci.* 18, 515–529. <https://doi.org/10.5194/nhess-18-515-2018>.
- Pivello, V.R., 2011. The use of fire in the cerrado and amazonian rainforests of Brazil: past and present. *Fire Ecol.* 7, 24–39. <https://doi.org/10.4996/fireecology.0701024>.
- Programa Queimadas INPE, 2018. Área Queimada Resolução 1 km [WWW Document]. URL <http://prodwww-queimadas.dgi.inpe.br/aq1km/>
- Ramos-Neto, M.B., Pivello, V.R., 2000. Lightning Fires in a Brazilian Savanna National Park: Rethinking Management Strategies. <https://doi.org/10.1007/s002670010124>.
- Rummukainen, M., 2010. State-of-the-art with regional climate models. *Wiley Interdiscip. Rev. Clim. Chang.* 1, 82–96. <https://doi.org/10.1002/wcc.8>.
- Rusticucci, M., 2012. Observed and simulated variability of extreme temperature events over South America. *Atmos. Res.* 106, 1–17. <https://doi.org/10.1016/j.jatmosres.2011.11.001>.
- Samuelsson, P., Gollvik, S., Jansson, C., Kupiainen, M., Kourzeneva, E., Van De Berg, W.J., 2015. The surface processes of the Rossby Centre regional atmospheric climate model (RCA4). *Meteorologi.*
- Samuelsson, P., Jones, C.G., Will'En, U., Ullerstig, A., Gollvik, S., Hansson, U., Jansson, E., Kjellström, C., Nikulin, G., Wyser, K., 2011. The Rossby centre regional climate model RCA3: model description and performance. *Tellus A Dyn. Meteorol. Oceanogr.* 63, 4–23. <https://doi.org/10.1111/j.1600-0870.2010.00478.x>.
- Schmidt, I.B., Moura, L.C., Ferreira, M.C., Eloy, L., Sampaio, A.B., Dias, P.A., Berlinck, C.N., 2018. Fire management in the Brazilian savanna: First steps and the way forward. *J. Appl. Ecol.* 55, 2094–2101. <https://doi.org/10.1111/1365-2664.13118>.
- Shlisky, A., Meyer, R., Waugh, J., Blankenship, K., 2008. *Fire, Nature, and Humans: Global Challenges for Conservation*. Fire Manage. today.
- Silva, P., Bastos, A., DaCamara, C.C., Libonati, R., 2016. Future projections of fire occurrence in Brazil using EC-earth climate model. *Rev. Bras. Meteorol.* 31, 288–297. <https://doi.org/10.1590/0102-778631320150142>.
- Solman, S.A., Blázquez, J., 2019. Multiscale precipitation variability over South America: Analysis of the added value of CORDEX RCM simulations. *Clim. Dyn.* 1–19. <https://doi.org/10.1007/s00382-019-04689-1>.
- Sterl, A., Bintanja, R., Brodeau, L., Gleeson, E., Koenigk, T., Schmith, T., Semmler, T., Severijns, C., Wyser, K., Yang, S., 2012. A look at the ocean in the EC-Earth climate model. *Clim. Dyn.* 39, 2631–2657. <https://doi.org/10.1007/s00382-011-1239-2>.
- Strandberg, G., Barring, L., Hansson, U., Jansson, C., Jones, C., Kjellström, E., Kolax, M., Kupiainen, M., Nikulin, G., Samuelsson, P., Ullerstig, A., Wang, S., 2014. CORDEX scenarios for Europe from the Rossby Centre regional climate model RCA4, Report Meteorology And Climatology.
- Strassburg, B.B.N., Brooks, T., Feltran-Barbieri, R., Iribarrem, A., Crouzeilles, R., Loyola, R., Latawiec, A.E., Oliveira Filho, F.J.B., Scaramuzza, C.A.de.M., Scarano, F.R., Soares-Filho, B., Balmford, A., 2017. Moment of truth for the Cerrado hotspot. *Nat. Ecol. Evol.* 1, 0099. <https://doi.org/10.1038/s41559-017-0099>.
- Sulla-Menashe, D., Friedl, M.A., 2018. User Guide to Collection 6 MODIS Land Cover (MCD12Q1 and MCD12C1) Product. <https://doi.org/10.5067/MODIS/MCD12Q1>.
- Taylor, S.W., Alexander, M.E., 2006. Science, technology, and human factors in fire danger rating: the Canadian experience. *Int. J. Wildl. Fire* 15, 121. <https://doi.org/10.1071/WF05021>.
- Torralba, V., Doblas-Reyes, F.J., Gonzalez-Reviriego, N., 2017. Uncertainty in recent near-surface wind speed trends: a global reanalysis intercomparison. *Environ. Res. Lett.* 12, 114019. <https://doi.org/10.1088/1748-9326/aa8a58>.
- Trenberth, K.E., Fasullo, J.T., Mackaro, J., 2011. Atmospheric moisture transports from ocean to land and global energy flows in reanalyses. *J. Clim.* 24, 4907–4924. <https://doi.org/10.1175/2011JCLI4171.1>.
- UNFCCC, 2015. Paris Agreement.
- van der Werf, G.R., Randerson, J.T., Giglio, L., van Leeuwen, T.T., Chen, Y., Rogers, B.M., Mu, M., van Marle, M.J.E., Morton, D.C., Collatz, G.J., Yokelson, R.J., Kasibhatla, P.S., 2017. Global fire emissions estimates during 1997–2016. *Earth Syst. Sci. Data* 9, 697–720. <https://doi.org/10.5194/essd-9-697-2017>.
- van Vuuren, D.P., Edmonds, J., Kainuma, M., Riahi, K., Thomson, A., Hibbard, K., Hurtt, G.C., Kram, T., Krey, V., Lamarque, J.-F., Masui, T., Meinshausen, M., Nakicenovic, N., Smith, S.J., Rose, S.K., 2011. The representative concentration pathways: an overview. *Clim. Change* 109, 5–31. <https://doi.org/10.1007/s10584-011-0148-z>.
- Van Wagner, C.E., 1987. Development and structure of the Canadian Forest Fire Weather Index System. Canadian Forestry Service.
- Westerling, A.L., Hidalgo, H.G., Cayan, D.R., Swetnam, T.W., 2006. Warming and Earlier Spring Increase Western U.S. Forest Wildfire Activity. *Science* (80-) 313, 940–943. <https://doi.org/10.1126/science.1128834>.
- Wilks, D.S., 2011. *Statistical Methods in the Atmospheric Sciences*. Elsevier/Academic Press.
- Wu, M., Schurgers, G., Ahlström, A., Rummukainen, M., Miller, P.A., Smith, B., May, W., 2017. Impacts of land use on climate and ecosystem productivity over the Amazon and the South American continent. *Environ. Res. Lett.* 12, 054016. <https://doi.org/10.1088/1748-9326/aa6fd6>.
- Wuyts, B., Champneys, A.R., House, J.I., 2017. Amazonian forest-savanna bistability and human impact. *Nat. Commun.* 8, 15519. <https://doi.org/10.1038/ncomms15519>.
- Zalles, V., Hansen, M.C., Potapov, P.V., Stehman, S.V., Tyukavina, A., Pickens, A., Song, X.-P., Adusei, B., Okpa, C., Aguilar, R., John, N., Chavez, S., 2019. Near doubling of Brazil's intensive row crop area since 2000. *Proc. Natl. Acad. Sci.* 116, 428–435. <https://doi.org/10.1073/PNAS.1810301115>.